Influence of vibrational excitation and collision energy on the ion-molecule reaction $NH_3^+(\nu_2)+ND_3$

Lynmarie A. Posey,[a] Robert D. Guettler, Nicholas J. Kirchner,[b] and Richard N. Zare[c]
Department of Chemistry, Stanford University, Stanford, California 94305

(Received 16 March 1994; accepted 13 May 1994)

The influence of vibrational excitation and collision energy on the ion-molecule reaction $NH_3^+(\nu_2)+ND_3$ has been investigated using a recently constructed quadrupole-octopole-quadrupole mass spectrometer. The NH_3^+ reagent ions are prepared state selectively with 0–7 quanta in the ν_2 umbrella bending mode by (2+1) resonance enhanced multiphoton ionization through the $\tilde{B}$ or $\tilde{C}'$ Rydberg states of ammonia. Reactive collisions between the mass-filtered ion beam and a thermal distribution of neutral reagent molecules occur with controlled collision energies (0.5–10.0 eV center of mass) within the octopole ion guide, enabling product ions to be collected independent of scattering dynamics. The reaction of NH_3^+ with ND_3 has three major product channels: (1) deuterium abstraction, (2) charge transfer, and (3) proton transfer. Each of these channels exhibits a strong dependence on ion vibrational excitation and collision energy. Product branching ratios and relative cross sections are reported and compared with previous results. Briefly, both deuterium abstraction and charge transfer are enhanced by vibrational excitation, whereas proton transfer is suppressed. As the collision energy increases, the branching fraction for charge transfer increases sharply, that for proton transfer decreases, and that for deuterium abstraction remains nearly unchanged. These results point to a short-lived collision complex in which vibration and translation play inequivalent roles.

I. INTRODUCTION

In attempting to understand reaction processes at a more fundamental level, chemists prepare known reactant states and determine the resulting product branching ratios and distributions of product states. State-to-state studies of dynamics are well-known for neutral–neutral reactions but much less so for ion-molecule reactions. The ease of charged particle manipulation, such as velocity control and charged particle detection, is a significant advantage in the study of ion-molecule reactions. However, with charged particles, the strong ion-dipole or ion-induced dipole forces present can so dominate the reaction dynamics that more subtle features of interest are hidden, limiting the accessible information. In this paper we study a particular ion-molecule reaction, $NH_3^+(\nu_2)+ND_3$, in which we can control the internal and translational energies of the reagent ion and measure their influence on the product channels identified by mass spectrometry. We find that despite the charged particle effects, the product branching ratios and cross sections are sensitive functions of reagent internal and translational energy, revealing a rich competition between different factors influencing the outcome of a reactive collision event.

One- or multiple-photon ionization is typically used to produce cationic reagents for ion-molecule studies of the influence of internal excitation on reactivity.[1] In such studies the photoelectron energy distribution serves as a diagnostic label for the internal energy of the resulting ion. Coincidence detection of photoelectrons produced by one-photon ionization and product ion signals has been widely employed to study the reactivity of ions with controlled internal energy.[2,3] Preparation with vibrational[4–11] and even rotational[12,13] selectivity has been achieved using $(n+1)$ resonance enhanced multiphoton ionization (REMPI). These ionization techniques can often allow access to a wider range of internal energies than is typically available with neutral reagents, provided a significant change in geometry occurs in going from the ground state of the neutral molecule to the ground state of the ion. In neutral systems, studies of the reactivity of vibrationally excited neutral reagents can be complicated by reaction of unexcited neutrals that remain in the ground state; this problem is overcome for positively charged ionic reagents because only those molecules that actually absorb a photon produce ionic reagents. Although ionization presents some definite advantages in preparing vibrationally and rotationally excited reagents, ionization, in general, does not produce high concentrations of reagents, making state-to-state measurements difficult[14–17] and for many systems impossible. Ionic reagents, by virtue of their charge, also allow access to a much greater range of collision energies than techniques typically used in neutral reaction studies, such as molecular beam seeding or fast atom production by photodissociation.

Over the past ten years a growing number of research groups have adopted radio-frequency (rf) ion-guide techniques for studying ion-molecule reactions;[18–22] much of this work has been reviewed in a recent article by Gerlich.[23] The use of guided ion beam techniques for the measurement of integral cross sections in ion-molecule reactions was pioneered by Teloy and Gerlich[24] over fifteen years ago. In subsequent work, Anderson *et al.*[18] first coupled state-selective one-photon VUV ion preparation with guided ion techniques

[a]Current address: Department of Chemistry, Vanderbilt University, Nashville, Tennessee 37235.
[b]Current address: Massively Parallel Instruments, Inc., 2030 Fortune Drive, Suite A, San Jose, California 95131.
[c]Author to whom all correspondence should be directed. E-mail: rnz@chemistry.Stanford.EDU

 0021-9606/94/101(5)/3772/15/$6.00

in their study of the effects of vibrational excitation and translational energy on the dynamics of the reaction $H_2^+ + H_2$ and its isotopic variants. Shao and Ng[20,25] extended the work on the state-selected reactivity of the $H_2^+ + H_2$ system using a quadrupole-octopole-quadrupole mass spectrometer; addition of the quadrupole mass filter prior to the rf-only octopole allowed the reaction to be studied without isotopic labeling. With the addition of a second octopole ion-guide and third quadrupole mass filter Ng and co-workers[16] have also been able to measure absolute state-to-state cross sections using differential reactivity to probe the ionic product state distributions. Another approach to product state detection in an rf guided ion beam instrument was demonstrated by Scherbarth and Gerlich,[26] who used laser-induced photodissociation to examine O_2^+ product state distributions in the charge transfer reaction $Ar^+ + O_2$ carried out at center-of-mass collision energies as low as 0.04 eV. In this study Scherbarth and Gerlich also extracted kinetic energy release information from the product ion time-of-flight profiles. Anderson and co-workers[27–29] have recently coupled state-selective preparation of molecular ions using multiphoton ionization (MPI) as a reagent ion source with a guided ion beam mass spectrometer to study the reactivity of $C_2H_2^+$ and OCS^+ ions. In addition to their use in measurements of reactive cross sections for atomic and molecular ions, rf octopole ion guides have been used to study collision induced dissociation[30,31] and reactions of ionic clusters.[32–34] The work mentioned earlier represents only a sampling of the applications of guided ion beam techniques.

The reaction of the ammoniumyl ion, NH_3^+, with ammonia was one of the first ion-molecule reactions in which the influence of vibrational excitation on the reaction outcome was investigated. This system is truly ideal for investigating the influence of reactant ion internal excitation because the large change in geometry in going from the ground state of the neutral to the ground state of the ion (pyramidal→planar) allows ions to be produced with as many as 13 quanta (1.66 eV) in the ν_2 umbrella bending mode.[35,36] In pioneering work Chupka and Russell[37] used one-photon VUV photoionization to produce $NH_3^+(\nu_2=0-10)$ and investigated the $NH_3^+(\nu_2)+NH_3$ reaction. They observed that the relative cross section for the formation of NH_4^+ decreases by a factor of 2 as the vibrational excitation was increased from $\nu_2=0-10$. This reaction

$$NH_3^+ + NH_3 \rightarrow NH_4^+ + NH_2 \qquad (1)$$

is strongly exothermic, $\Delta H=-0.9\pm0.2$ eV (Refs. 38–45) and proceeds at the collision limit predicted by average dipole orientation theory (ADO) (Ref. 46) under thermal conditions ($k=2.1-2.5\times10^{-9}$ cm^3 s^{-1} molecule^{-1}) (Refs. 40, 41, and 47). Chupka and Russell proposed that the reaction of NH_3^+ with NH_3 proceeds through a long-lived intermediate complex. They presented statistical arguments that the decrease in NH_4^+ formation with increasing internal excitation was caused by competition of the NH_4^+ channel with both charge transfer and decomposition of the $NH_3^+ \cdot NH_3$ complex to its original reagents. Several years later Chesnavich and Bowers[48] carried out phase space calculations for this reaction system and found poor agreement with the experimental results of Chupka and Russell leading Chesnavich and Bowers to suggest that this reaction is nonstatistical.

The thermoneutral charge transfer reaction produces NH_3^+ product ions that cannot be differentiated from unreacted NH_3^+ ions in many experiments. Huntress *et al.*[49] used ^{15}N labeled NH_3 to probe the relative rates for formation of the charge transfer and NH_4^+ products in nonstate-selected ion cyclotron resonance (ICR) experiments over collision energies ranging from thermal to 50 eV. They found that the charge transfer rate at thermal energies was negligibly small but increased with kinetic energy while the proton transfer rate dropped. Closer examination of the system also reveals two possible mechanisms for formation of NH_4^+, proton transfer and hydrogen atom abstraction, which are indistinguishable without isotopic labeling of either the ionic or neutral reagent. Using a mixture of ^{15}N and ^{14}N labeled NH_3^+ Huntress and Pinizzotto[39] determined the relative rates for hydrogen atom abstraction and proton transfer, k_{HAA}/k_{PT} to be 0.28 ± 0.04, at thermal collision energies. In the same paper these authors also report that the rate constant for reaction (1) falls as the energy of the ionizing electrons is increased and, hence, the internal energy of the resulting reagent ions is increased. A similar dependence of rate constants on internal energy was obtained by Sieck, Hellner, and Gorden[50] using direct one-photon VUV photoionization to prepare NH_3^+ in the vibrational ground state ($k=2.3\times10^{-9}$ cm^3 s^{-1} molecule^{-1}) and with vibrational excitation. Further evidence for the presence of hydrogen atom abstraction as well as proton transfer channels was provided by the selected ion flow tube (SIFT) experiments of Adams *et al.*;[47] in reactions of ND_3^+ with NH_3 they observed a branching ratio between the deuteron transfer and the hydrogen atom abstraction channels of 17:3. Adams *et al.* noted that although hydrogen atom abstraction is an exothermic process in the reactions of NH_3^+ with H_2O and H_2, in both cases the rate is significantly smaller than the Langevin or ADO collision rates.

Baer and Murray[51] were the first to look at the influence of both vibrational excitation and collision energy on the charge transfer channel as well as proton transfer, using time of flight (TOF) to distinguish between product ions and unreacted NH_3^+ in a photoion-photoelectron coincidence (PIPECO) experiment. Their observation of a decreasing proton transfer cross section with increasing vibrational excitation at collision energies of 0.1–1.0 eV corroborated the earlier results of Chupka and Russell.[37] Baer and Murray also investigated the influence of collision energy on proton transfer. The cross section decreased with increasing collision energy as expected; however, at low collision energies the cross section for proton transfer was greater than that predicted by Langevin or ADO theory whereas at collision energies greater than 0.5 eV it was less than that predicted by either theory. This behavior argued against the reaction proceeding exclusively through a long-lived intermediate. In contrast, the charge transfer cross section increased with vibrational excitation, although the change in cross sections with ν_2 was not nearly so large as the change in Franck–Condon factors between $\nu_2=0$ and $\nu_2\geqslant1$. Baer and Murray developed a semiquantitative impact parameter model to de-

scribe the observed behavior. This model classified collisions leading to charge transfer as either intimate or large impact parameter interactions. They suggested that vibrational excitation of the reagent ion was only important in collisions with an impact parameter exceeding the Langevin orbiting impact parameter.

Subsequent PIPECO experiments carried out by van Pijkeren *et al.*[43] at thermal collision energies confirmed that proton transfer is suppressed by vibrational excitation. Statistical modeling of this data suggested that a limited number of internal degrees of freedom participate in energy redistribution within the intermediate complex. These authors also state that dynamical constraints on the proton transfer reaction become more important as the collision energy is raised from thermal to 1 eV based on their results and those of Baer and Murray.[51]

As mentioned earlier, without isotopic labeling of either the ionic or neutral reagent in the ammoniumyl ion/ammonia system it is impossible to distinguish between proton transfer and hydrogen atom abstraction, and charge transfer can only be studied with difficulty. Previously in this laboratory, Conaway *et al.*[44] studied two isotopic variants of this system: $NH_3^+ + ND_3$ and $ND_3^+ + NH_3$ as a function of vibrational excitation in the ν_2 umbrella bending mode of the ion and collision energy. The reagent NH_3^+ and ND_3^+ were prepared in a state-selective manner with 0–10 quanta in the ν_2 mode using (2+1) REMPI through either the $\tilde{B}$ or $\tilde{C}'$ Rydberg states.[5] The experiments were carried out using a tandem quadrupole mass spectrometer with a static collision cell located between the two quadrupole mass analyzers. Conaway *et al.*[44] found that neutral atom abstraction was enhanced by as much as a factor of 6, charge transfer increased by factor of 2, and proton/deuteron transfer decreased by a factor of 2 as the vibrational excitation in the umbrella mode was increased from $\nu_2=0$ to $\nu_2=10$. These results led them to propose a simple model to explain the behavior of this ion-molecule reaction system. They suggested that the vibrational motion in the ν_2 mode, which corresponds to motion along the reaction coordinate for neutral atom abstraction, promotes this reaction channel; this same motion is orthogonal to the reaction coordinate for proton/deuteron transfer and suppresses the process.

The experimental configuration used by Conaway *et al.*[44] unfortunately precluded direct comparison of the signal arising from different product channels and, hence, the measurement of product branching ratios and reaction cross sections because forward-scattered product ions were detected more efficiently than side- and back-scattered products. Consequently, their work was limited to exploring the influence of vibrational excitation and collision energy within a given product channel, and it was impossible to explore the subtle interplay between the three major product channels for this ion-molecule reaction. Tomoda, Suzuki, and Koyano[45(a)] subsequently measured relative cross sections for the three major product channels of the reactions $NH_3^+(\nu_2=4, 6, 8, 11)+ND_3$ and $ND_3^+(\nu_2=4, 6, 9, 12)+NH_3$ over center-of-mass (c.m.) collision energies ranging from 0.9–4.5 eV using threshold electron secondary ion coincidence (TESICO). Their measurements showed general agreement with the trends observed by Conaway *et al.* Tomoda *et al.* invoked a model based upon nonadiabatic transition theory to explain the observed behavior; they suggested that H/D atom abstraction could actually be viewed as stepwise electron transfer followed by H^+/D^+ transfer.[45]

In this paper we report relative cross sections and product branching ratios for the ion-molecule reaction

$$NH_3^+(\nu_2=0\text{–}7)+ND_3 \rightarrow NH_3D^+ + ND_2 \quad \text{(deuterium abstraction)} \tag{2a}$$

$$\rightarrow NH_3 + ND_3^+ \quad \text{(charge transfer)} \tag{2b}$$

$$\rightarrow NH_2 + ND_3H^+ \quad \text{(proton transfer)} \tag{2c}$$

measured at c.m. collision energies ranging from 0.5–10.0 eV using a recently constructed quadrupole-octopole-quadrupole instrument that incorporates laser multiphoton ionization to prepare reagent ions in selected levels of the ν_2 umbrella bending mode. A detailed description of this instrument is provided in the previous article.[52] The octopole ion guide was added to the collision cell region of the tandem quadrupole apparatus used previously by Conaway *et al.*[44] to improve product ion collection efficiency and to remove dynamics-dependent discrimination in product ion detection inherent in the static collision cell design. Our relative cross section and product branching ratios extend the previous work on this ion-molecule reaction system. In addition, direct comparison of our results with TESICO data of Tomoda *et al.*[45] and PIPECO results of Baer and Murray[51] allows us to evaluate the performance of this instrument. Models to explain the experimentally observed behavior are proposed.

II. EXPERIMENT

The quadrupole-octopole-quadrupole mass spectrometer (Fig. 1) used in this work to investigate the roles of vibrational excitation and collision energy in the ion-molecule reaction $NH_3^+(\nu_2=0\text{–}7)+ND_3$ is described in detail in the previous article on the $N^+ + O_2$ ion-molecule system.[52] The most significant difference between the two studies is the ionization scheme used to generate the reactant ions. The previous study used electron impact ionization to generate the N^+ reactant ions, whereas this study uses REMPI to prepare the NH_3^+ reactant ions in a state-selective manner. The state selection requires some additional procedures that are described below along with the details of the photoionization method.

We begin with a general overview of the instrument. Reagent ions are prepared with vibrational state selectivity by (2+1) REMPI in a pulsed molecular beam of ammonia. The resulting ions are then focused and injected into the first quadrupole mass filter, which removes any ionic fragments produced in the ionization process. After acceleration to the desired kinetic energy, the ion beam enters the rf octopole ion guide,[18–22,24] into which the neutral target gas is admitted. The unreacted reagent ions and product ions are guided

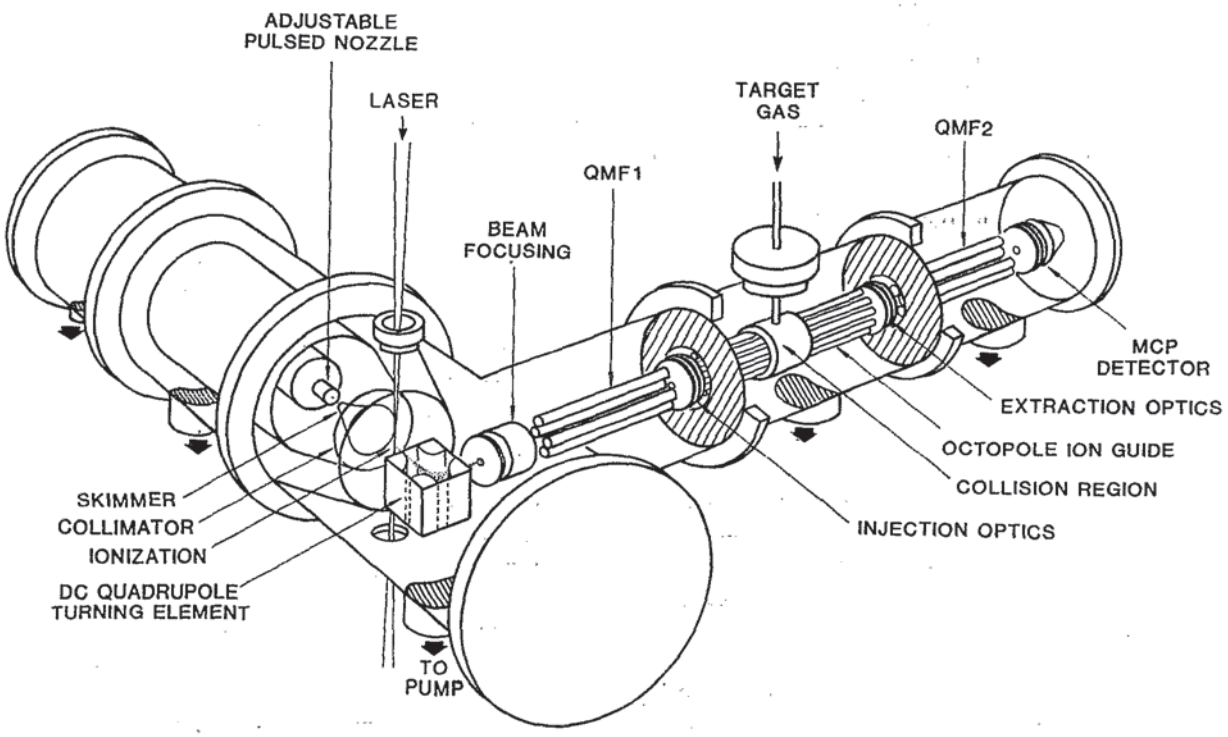

FIG. 1. Schematic illustration of the quadrupole-octopole-quadrupole mass spectrometer employed to study ion-molecule reactions with state-selective preparation of the reagent ions by resonance enhanced multiphoton ionization. (QMF is the quadrupole mass filter, MCP is the microchannel plate.)

by the octopole to the second quadrupole for mass analysis and subsequent detection. The product and reactant ion intensities are used to calculate product branching ratios and relative cross sections, which are monitored as both the reagent ion kinetic energy and vibrational excitation are varied.

A. Laser photoionization source

The laser photoionization source used to generate the NH_3^+ reactant ion beam consists of a pulsed molecular beam and a pulsed (10 Hz) frequency-doubled Nd:YAG-pumped dye laser (Quanta Ray DCR-1A, PDL-1, WEX). The molecular beam composition is 10% NH_3 (Liquid Carbonic, anhydrous NH_3, 99.99%) seeded in He (Liquid Carbonic, 99.995%). The ionizing UV laser beam (275–340 nm, 4–15 mJ/pulse) is focused with an $f=250$ mm lens and intersects the molecular beam approximately 1.7 cm beyond the molecular beam collimating plate in a vacuum chamber maintained at 3×10^{-7} Torr.

The $NH_3^+(\nu_2)$ reagent ions are selectively prepared with excitation in the umbrella bending mode using (2+1) REMPI through either the $\tilde{B}$ or $\tilde{C}'$ Rydberg states. Previous photoelectron spectroscopy (PES) measurements[5] have shown that one-photon ionization from these intermediate Rydberg states, which have nearly the same equilibrium geometry as the ionic ground state, favors the $\Delta\nu=0$ transition, producing NH_3^+ with vibrational state selectivity ranging from 74%–100 %. Because of the large change in geometry in going from the pyramidal neutral to the planar ion, NH_3^+ photoions can be prepared with up to 10 quanta in the ν_2 umbrella mode, which corresponds to 1.25 eV (Ref. 36) of internal excitation.

B. Quadrupole-octopole-quadrupole mass spectrometer

The instrument configuration presented in the previous paper[52] is unchanged for this photoionization work, although some additional features were used. The laser crosses the molecular beam ~1 cm downstream from the point where electron impact ionization occurred. The ions produced by the laser travel with the molecular beam for approximately 1.5 cm (<10 μs) before being deflected at right angles onto the ion beam axis by a dc quadrupole turning element.[53–55] At the point in the molecular beam expansion where ionization occurs, collisions have ceased. Any collisions that occur between the vibrationally state selected NH_3^+ ions and the helium carrier gas as the ions are extracted from the molecular beam should not perturb the vibrational state-selection because helium is an inefficient collider for vibrational relaxation. Because the ionizing laser and molecular beam are both pulsed, no ion beam chopping is required to eliminate background ions.

Nominal collision energies are determined by the potential difference between the laser ionization region and the octopole float voltage. We studied the $NH_3^+ + ND_3$ reaction at collision energies of 0.5–10.0 eV in the center-of-mass frame (0.93–18.50 eV lab frame). At the lowest collision energy studied, 0.5 eV c.m. the $NH_3^+(\nu_2)$ will exit the octo-

pole less than 150 μs after it is state-selectively prepared by (2+1) REMPI. Mauclaire *et al.*[56] have obtained qualitative results indicating that NH_3^+ ions produced in highly excited umbrella bending mode (ν_2) levels of the ground electronic state have lifetimes of 10–20 ms with respect to radiative relaxation and internal conversion to the long-lived stretching mode (τ>300 ms). Hence, relaxation of the vibrationally excited reagent ions is unimportant on the time scale of our experiment.

The flow of the neutral collision gas, ND_3 (Cambridge Isotopes Laboratory 99.5% or MSD Isotopes 99.1%), leading to the leak valve is regulated to maintain a backing pressure of 15 psi. The pressure in the line leading from the leak valve to the collision cell is maintained at 1 Torr, which causes a pressure of 1×10^{-6} Torr in the vacuum chamber containing the octopole and collision cell (base pressure 2×10^{-7} Torr). The geometry of the octopole precludes an accurate determination of the actual cell length, and accurate pressure measurements in the region are difficult. Therefore, we currently do not attempt to measure absolute cross sections but report instead relative cross sections for the major product channels.

Single-collision conditions are ensured by monitoring the ionic product of the secondary reaction between the charge transfer product and the neutral target gas

$$ND_3^+ + ND_3 \rightarrow ND_4^+ + ND_2. \tag{3}$$

The resulting ND_4^+ (m/e=22 a.m.u.) signal decreases with decreasing pressure and levels off at 2%–3% of the product signal. The pressure dependence and TOF profile for the m/e =22 a.m.u. signal are consistent with formation of a secondary product ion. Measurements are made at the lowest collision gas pressure possible while maintaining reasonable signal levels. The secondary reaction (3) has a larger cross section than the primary reaction channels (2) because the kinetic energy of the ionic reagent ND_3^+ is lower than the main ion beam of NH_3^+; as a result, the ND_4^+ product cannot be totally eliminated. The total product ion signal under our operating collision gas pressures is less than 1% of reagent ion beam signal. The main reagent beam is attenuated by less than 10% when the neutral target gas is introduced to the collision region.

As described in the $N^+ + O_2$ experimental section,[52] the combined analog and ion counting schemes provide the capability to measure ion intensities of greatly varying magnitude. The output from the chevron microchannel plate ion detector (Galileo Electro-Optics FTD-2003) is fed to a dual output preamplifier (LeCroy 612A); one output connects to the analog detection electronics and the other output connects to the ion counting electronics. In the analog detection scheme, a slow amplifier/integrator (EG&G Ortec 474) receives the output of the preamplifier. The amplified and integrated signal is fed into a transient digitizer (LeCroy TR8837F). The transient digitizer is located in a CAMAC Crate (Kinetics Systems, Model 1502), which is interfaced to a digital computer (486–33 MHz IBM compatible). The digitizer is read out by the computer on a shot-to-shot basis. The ion counting is accomplished by first discriminating (LeCroy 4608C) the output of the preamplifier, and taking the discriminator output into a multichannel scalar (home built with DSP QS-450 100 MHz quad scalar front end). The scalar is connected to the CAMAC Crate and, hence, to the computer. The reagent ion peak intensity (50–200 ion counts per laser shot) is too large to measure with ion counting and, hence, is measured with the analog detection scheme, while the significantly weaker product signal (<0.1 counts/shot) is detected by ion counting. All data acquisition is computer controlled using the CAMAC interface.

Raw data are recorded as time-of-flight profiles (see Figs. 3 and 4, *vide infra*). The TOF profiles have proven to be an indispensable tool in optimizing and diagnosing machine conditions. The reagent ion TOF profile is used to optimize the source conditions and the ion optics voltages. All settings are adjusted to yield the maximum TOF profile height, which occurs simultaneously with the narrowest profile width, resulting in the greatest number of reagent ions with the least amount of perturbation to the ion packet.

Using the octopole ion guide to transport the unreacted reagent ions and product ions to the second quadrupole mass filter eliminates the discrimination in product detection that hindered previous state-selected ion-molecule reaction studies in this laboratory.[6,44,57–59] As a result, the present study can determine product branching ratios and relative cross sections, quantities that require direct comparison between different product channels.

In the study of the $N^+ + O_2$ reaction system with the current instrument,[52] the reagent N^+ ion beam kinetic energy spread was characterized and its effect on the overall collision energy uncertainty was discussed. Much of that characterization and discussion is directly applicable to this $NH_3^+ + ND_3$ study and will be briefly summarized. The reagent ion kinetic energy has two components: a radial component, orthogonal to the ion beam axis, and an axial component, parallel to the ion beam axis. The radial component of the velocity spread arises primarily from the interaction of the reagent NH_3^+ ions with the rf potentials in the first quadrupole and the octopole ion guide. The axial component of the velocity spread arises from convolution of the initial velocity spread of the ionized molecules with the overall instrument function, which includes the interaction of the ions with the static optics and rf fringing fields.

The ion trajectory simulations discussed in the previous article[52] showed that most of the variation in radial kinetic energy of the NH_3^+ ions is caused by the range of positions with which the ion can enter the octopole; the larger the off-axis positions upon entering the octopole, the greater the radial kinetic energy component. The preceding paper found that (1) the radial energy spread in our apparatus is approximately independent of the axial energy of the ion, and (2) the radial energy spread is such that 50% of the time the ions have a radial energy less than 0.1 eV and 90% of the time less than 0.5 eV.

Summarizing the basic energy relationships for the $NH_3^+ + ND_3$ system, the center-of-mass collision energy is given by the expression

$$E_{\text{c.m.}} = \left(\frac{M}{m+M}\right) E_{\text{lab}} = 0.54 E_{\text{lab}}, \tag{4}$$

where E_{lab} is the kinetic energy in the lab frame, m is the mass of the reagent ion ($m=17$), and M is the mass of the thermal neutral reagent ($M=20$). The collision energy distribution, full width at half maximum,[60] is

$$\Delta E_{FWHM}=\left[11.1\left(\frac{m}{m+M}\right)kTE_{c.m.}\right]^{1/2}=0.36(E_{c.m.})^{1/2}, \tag{5}$$

neglecting any spread in the ion beam energy. At collision energies of 1.0 and 10.0 eV the collision energy spreads, ΔE_{FWHM}, are 0.36 and 1.14 eV, respectively.

In addition, we must also take into account the spread in the radial energy of the NH_3^+ in the octopole ion guide. This contribution is most significant at the lowest axial energies, which is typically a center-of-mass energy of 1.0 eV, corresponding to a laboratory energy of 1.8 eV. The estimates of the radial energy component obtained in the previous $N^+ + O_2$ study yield radial energies less than 0.5 eV 90% of the time. Adding this value (0.5 eV) to the worst case axial energy (1.8 eV) increases the collision energy ΔE_{FWHM} [Eq. (5)] by only 0.05 eV. Consequently, we conclude that the spread in the radial energy of the NH_3^+ ion seldom affects the value of the collision energy.

Using an instrument this complex to monitor and interpret variations in product channel intensities raises the issue of possible bias for or against the collection of particular product channels. The static optics that couple the octopole and the second quadrupole, the mass resolution of the second quadrupole, and the optics that couple the quadrupole and the detector are all potential sources of product ion discrimination. The extent of possible bias is difficult to accurately predict because of the number of variables that must be considered for each instrumental component involved, in conjunction with some knowledge of the product formation characteristics. Unfortunately, these product characteristics are often the objective of the measurement. A comprehensive check of all these influences can be accomplished by measuring the branching ratios for a well-characterized ion-molecule system that has characteristics similar to the systems of primary interest. Any discrepancies observed between the accepted and the measured branching ratios would indicate problems in product ion collection. We have carried out a comparison of this type using the ion-molecule reaction system $N^+ + O_2$, which is described in the preceding paper.[52] The comparison of the measured product branching ratios to the existing values revealed no significant discrimination in product ion detection above collision energies of 1.5 eV c.m. The ordering of the product ion intensities was correctly reproduced, and the largest difference between the two measurements was in the O_2^+ branching fraction, which we observed to be approximately 0.15 lower than the measurement of Neynaber *et al.*[61] With this comparison established, we can proceed with presentation and interpretation of the observed product ion intensities knowing the measurements have not been significantly tainted by instrumental discrimination for collision energies at least down to 1.5 eV c.m.

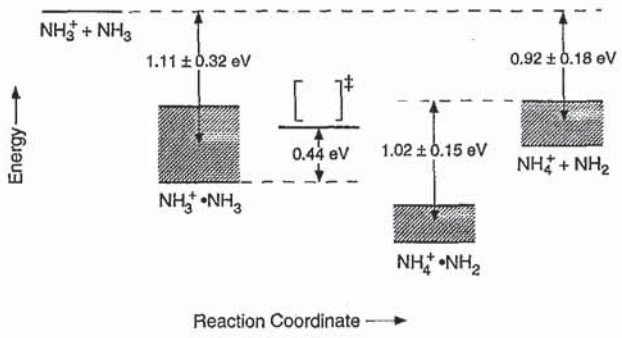

FIG. 2. Energetics for the $NH_3^+ + NH_3 \rightarrow NH_4^+ + NH_2$ reaction compiled from experimental and theoretical work (see text). The relative positions of reactant and product asymptotes, entrance and exit channel complexes, and the barrier between the entrance and exit channels are shown.

III. RESULTS

A. Energetics

To provide a framework for the discussion of the experimental results and the construction of models to explain the behavior of this system, Fig. 2 shows the relative energetics for the reactant and product asymptotes as well as the entrance and exit channel complexes for the reaction $NH_3^+ + NH_3 \rightarrow NH_4^+ + NH_2$. As mentioned in Sec. I, literature values for the overall reaction exothermicity range from -0.74 to -1.10 eV.[38–45] A binding energy of 0.79 ± 0.05 eV was determined for the $NH_3^+ \cdot NH_3$ entrance channel complex using one-photon molecular beam photoionization by Ceyer *et al.*[42] More recent photoionization measurements of Kamke *et al.*[62] suggest that the binding energy for this complex may be as high as 1.10 eV. The photoionization thresholds obtained for the $(NH_3)_2$ complex represent an upper limit for the adiabatic ionization energy and, as a result, the entrance complex binding energy calculated using this value is a lower limit. Calculations by Greer *et al.*[63] suggest that the measured ionization threshold corresponds to a nonvertical transition from the cyclic asymmetric neutral ammonia dimer to the hydrogen-bonded $NH_3^+ \cdot NH_3$ complex; they note that an additional 0.31 eV in excess of the photoionization energy is required to activate the intracluster proton transfer reaction

$$NH_3^+ \cdot NH_3 \rightarrow NH_4^+ + NH_2, \tag{6}$$

which is consistent with the experimentally observed appearance potential for NH_4^+ in dimer ionization studies.[62] *Ab initio* calculations by Radom and co-workers[64,65] suggest that the $NH_3^+ \cdot NH_3$ entrance channel complex may be as tightly bound as 1.43 eV with respect to the separated reagents. They predict a barrier to rearrangement from the entrance channel complex to the $NH_4^+ \cdot NH_2$ exit channel complex of 0.44 eV. Although the exit channel complex $NH_4^+ \cdot NH_2$ is thermodynamically more stable than the dimer $NH_3^+ \cdot NH_3$, an $N_2H_6^+$ species with two equivalent N's and six equivalent H's, apparently corresponding to the entrance channel com-

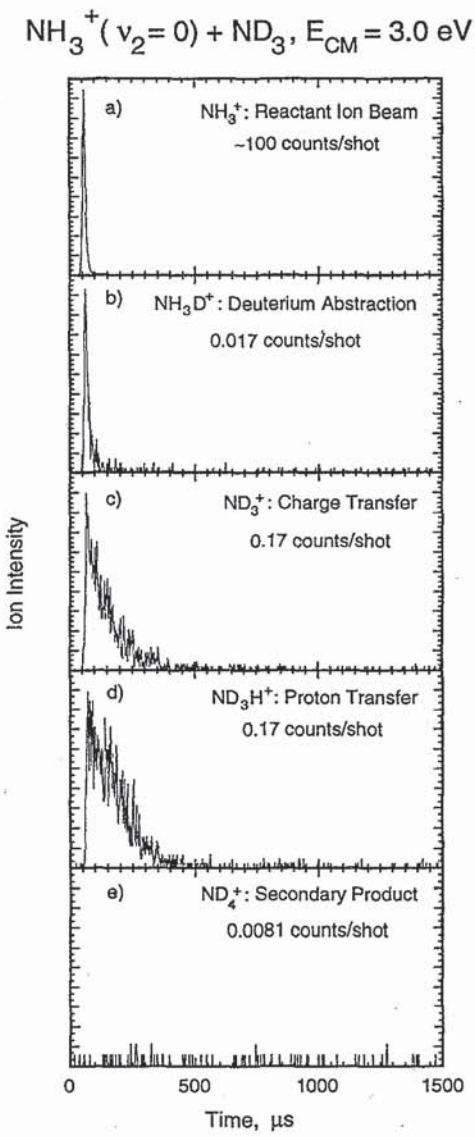

FIG. 3. Raw time-of-flight (TOF) spectra for (a) the unreacted reagent beam, $NH_3^+(\nu_2)$, and the three major product channels, (b) NH_3D^+, (c) ND_3^+, and (d) ND_3H^+, as well as (e) the secondary reaction product, ND_4^+. The data are for $NH_3^+(\nu_2=0)$ at a collision energy ($E_{c.m.}$) of 3.0 eV. The TOF profiles are arbitrarily normalized to highlight the profile shapes rather than the relative signal intensities. The average number of ion counts detected on each laser shot is indicated for each channel.

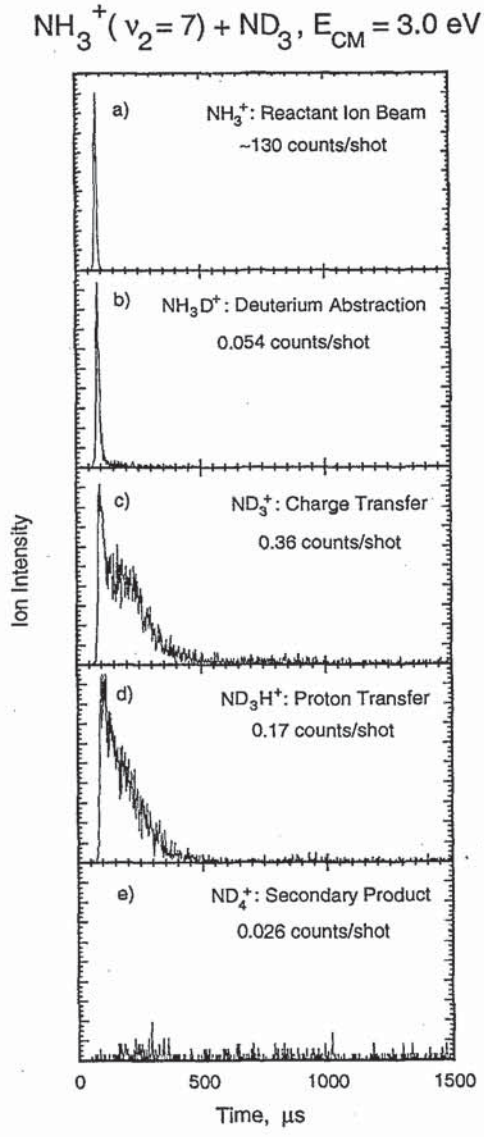

FIG. 4. Raw time-of-flight (TOF) spectra for (a) the unreacted reagent beam, $NH_3^+(\nu_2)$, and the three major product channels, (b) NH_3D^+, (c) ND_3^+, and (d) ND_3H^+, as well as (e) the secondary reaction product, ND_4^+. The data are for $NH_3^+(\nu_2=7)$ at a collision energy ($E_{c.m.}$) of 3.0 eV. The arbitrarily normalized TOF profiles highlight the profile shapes. The average number of ion counts detected on each laser shot is indicated for each channel.

plex, has been isolated in a matrix at 77 K.[66] *Ab initio* molecular orbital calculations by several groups[63–65,67–69] estimate the binding energy of the $NH_4^+ \cdot NH_2$ complex relative to the separated products at 0.87–1.17 eV.

Despite the spread in values given for these thermodynamic quantities, several trends are apparent from Fig. 2. The entrance and exit channel complexes, $NH_3^+ \cdot NH_3$ and $NH_4^+ \cdot NH_2$, are at least as stable thermodynamically as the reaction products and significantly more stable than the reagents in this exothermic reaction. In the absence of a significant barrier to reaction the entrance channel complex will not be stabilized under single-collision conditions and will proceed directly to products. Comparison of thermal rate constants with collision rate constants calculated using ADO and ADO with conservation of angular momentum (AADO) theories[40,46] indicates that reaction of the ammoniumyl ion with ammonia proceeds on nearly every collision, suggesting that no significant dynamical barrier to reaction exists. This observation is consistent with the *ab initio* prediction[64,65] that the barrier to rearrangement from the entrance channel complex, $NH_3^+ \cdot NH_3$, to the exit channel complex, $NH_4^+ \cdot NH_2$, is located roughly 1 eV below the asymptote for the separated reagents and 0.44 eV above the potential minimum corresponding to $NH_3^+ \cdot NH_3$.

B. Data

1. Characterization of product channels

Figures 3 and 4 present typical time-of-flight profiles for the different product channels as well as the primary ion beam. From such data product branching ratios and relative reaction cross sections are determined. The three primary product ion signals observed in our investigation of the reaction of state-selectively prepared NH_3^+ with ND_3 at collision energies of 0.5–10.0 eV c.m. occur at mass-to-charge (m/e) ratios of 19, 20, and 21. These features in the mass spectrum are assigned to the deuterium abstraction product NH_3D^+, the charge transfer product ND_3^+, and the proton transfer product ND_3H^+, respectively. Under all conditions these mass channels account for over 90% of the product ion signal measured. Along with these major channels there are two other low mass species occurring at $m/e=18$ and 22 that warrant discussion. The species with $m/e=22$ is thought to be the secondary reaction product ND_4^+, which was discussed previously in Sec. II. Evidence for this assignment includes the dependence of the signal intensity on the collision gas pressure and its TOF profile (see the following). Typically, this ionic species represents 2%–3% of the total product ion signal. A second minor feature appears in the mass spectrum at $m/e=18$ as the collision energy is increased. The TOF profile of this species is sharply peaked with roughly the same width as that of NH_3D^+ (see the following). We tentatively assign this species as NH_2D^+ formed by decomposition of the energized deuterium abstraction product, NH_3D^+. Loss of a D atom from this product is indistinguishable from the ionic reactant NH_3^+. At 3.0 eV collision energy the $m/e=18$ ion accounts for less than 2% of the product ions; at 10.0 eV, 5%–6% of the product signal arises from this feature.

In contrast to the previous work of Conaway *et al.*,[44] no condensation products were observed in the mass range $m/e=32$–36. Since the formation of protonated hydrazine ($N_2H_3D_2^+$ and $N_2H_2D_3^+$) is endothermic by 1.12 eV,[44] these products would be expected at higher collision energies based purely on energetic grounds. Conaway *et al.* observed masses at $m/e=35,36$, which they attributed to protonated hydrazine ions, and at higher energies they observed masses at $m/e=32$–34, which they interpreted as resulting from elimination of H_2, HD, and D_2 from the condensation complex $(NH_3\cdot ND_3)^+$. Protonated hydrazine ($N_2H_5^+$) formed in high pressure (0.01–1 Torr NH_3) electron impact ion sources has also been observed using mass spectrometry with a rate constant for formation of 1×10^{-11} cm^3 molecule^{-1} s^{-1}.[70,71] The branching ratio for this product increases sharply with pressure. Derwish and co-workers[70] suggest that the NH_3^+ reagent that forms protonated hydrazine may be electronically excited. Two possible explanations for the apparent absence of the high-mass products in our experiments are possible. In the previous work of Conaway and co-workers the pressures in the collision cell coupled with its length may not have been sufficiently low to ensure single-collision conditions; as a result, the condensation product could have been stabilized by a secondary collision. The secondary product ion, ND_4^+, was evident in the mass spectra for the $NH_3^+(\nu_2)+ND_3$ reaction obtained by Conaway *et al.* Although it was not possible to quantify the ND_4^+ signal with respect to the primary reaction products because of variation in product detection efficiencies, the presence of ND_4^+ in the mass spectra was significant. It is likely that this secondary reaction product was detected less efficiently than primary reaction products. For product ions to be detected in a tandem quadrupole apparatus with a static collision cell, they must have a significant velocity component in the laboratory frame directed toward the detector. Each reactive collision can reduce this velocity component and introduce off-axis components (see the discussion of time-of-flight data given later). In summary, detection of any ND_4^+ in the static cell configuration indicated a large number of secondary collisions. An alternative explanation for the absence of condensation products in this work is that the rate constant for this channel is too small for detection with our experimental apparatus. The product signal level under our current experimental conditions is sufficiently low (<1 product ion per laser shot) that we would expect to have some difficulty detecting product ions having rate constants for formation three orders of magnitude lower than the major product channels.

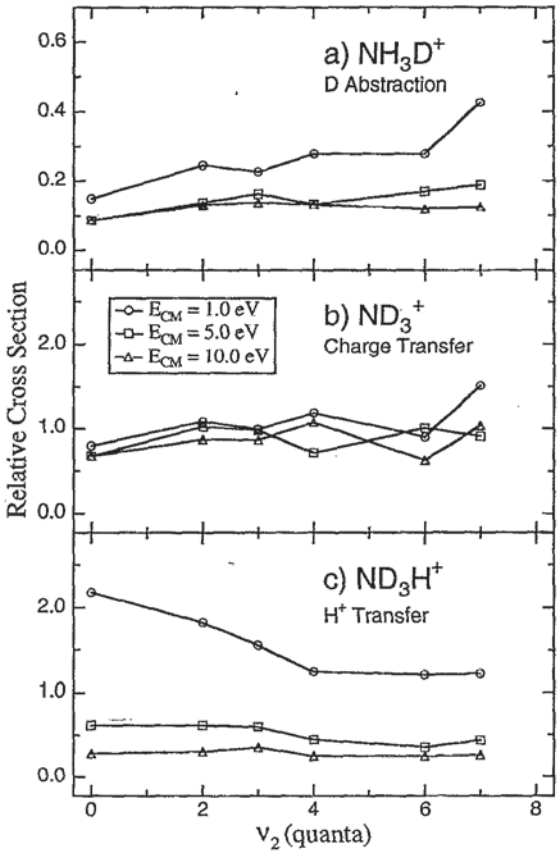

FIG. 5. Relative cross sections for each of the three major product channels in the reaction $NH_3^+(\nu_2=0$–$7)+ND_3$ plotted as a function of vibrational quanta in the ν_2 umbrella bending mode of NH_3^+ at three collision energies, $E_{c.m.}=1.0$, 5.0, and 10.0 eV.

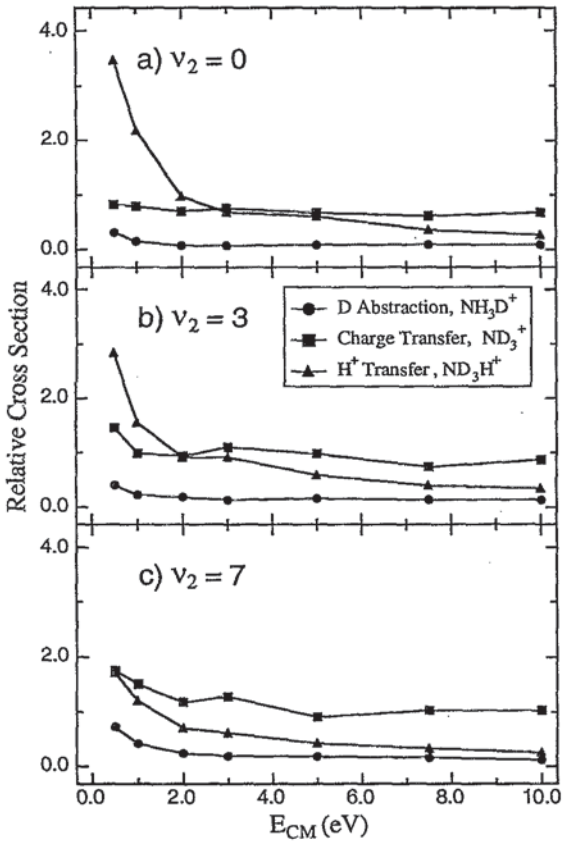

FIG. 6. Relative cross sections for the three major product channels in the reaction $NH_3^+(\nu_2)+ND_3$ plotted as a function of the center-of-mass collision energy, $E_{c.m.}$, at three umbrella mode excitations, $\nu_2=0$, 3, and 7.

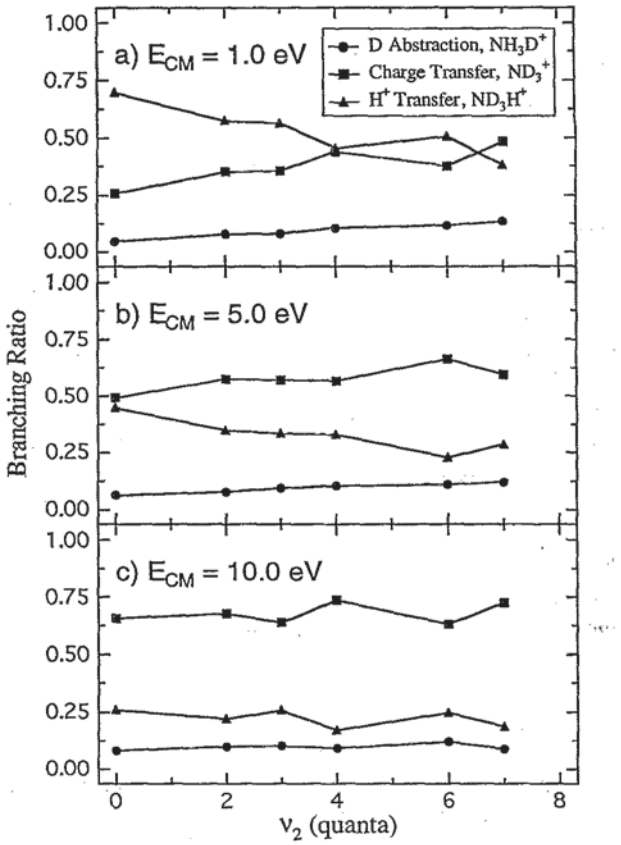

FIG. 7. Product branching ratios for the reaction $NH_3^+(\nu_2)+ND_3$ plotted as a function of ν_2 excitation at three center-of-mass collision energies, $E_{c.m.}$=1.0, 5.0, and 10.0 eV.

2. Time-of-flight profiles

Figures 3 and 4 show two typical sets of time-of-flight profiles for (a) the $NH_3^+(\nu_2)$ parent ion; the three major product channels, (b) deuterium abstraction, (c) charge transfer, and (d) proton transfer; and (e) the ND_4^+ secondary reaction product. These data are recorded for $\nu_2=0$ and $\nu_2=7$ at a center-of-mass collision energy of 3.0 eV. The TOF traces are arbitrarily normalized to highlight the shapes of the TOF profiles rather than the relative intensities of these features. In actuality, 100–150 $NH_3^+(\nu_2)$ ions are detected per laser shot, whereas less than one product ion per laser shot is recorded in all product channels.

Figures 3 and 4 show that fundamental differences exist between the product channel profiles. The TOF profiles reflect the projection of the product ion velocity vector on the ion beam axis of the instrument. These profiles can be used to examine the kinetic energy distributions of product ions as has been demonstrated by Scherbarth and Gerlich[26] in an investigation of energy partitioning in the reaction of $Ar^+ + O_2$ carried out in an rf ion guide and Dressler *et al.*[72] in their study of the reaction of N_2^+ with H_2O and D_2O in a thin, static collision cell. The TOF distribution of the NH_3D^+ deuterium abstraction product is only slightly broadened in comparison to the reactant ion beam. Qualitatively, it appears that the velocity vector of the reagent ion that abstracts a deuterium atom from the neutral ND_3 is relatively unchanged in the course of the reaction, which is consistent with the NH_3^+ ion "plucking" a deuterium atom from a neutral ND_3 molecule as it passes by without forming a long-lived intermediate complex. Little of the initial velocity of the reagent ion in the lab frame is lost to product recoil. In contrast, charge transfer and proton transfer, which result in the thermal neutral molecule becoming charged, have much broader TOF profiles. One possible explanation for these broadened TOF distributions is incomplete transfer of momentum to the thermal neutral reagent in the course of reaction. This explanation suggests a relatively short-lived complex leading to backscattering in the center-of-mass reference frame. Unlike the TOF profiles for the primary product ions, the TOF data for the $m/e=22$ ion (ND_4^+) shown in Figs. 3(e) and 4(e) are unstructured and extend well beyond the 2000 ms data collection window typically used. The abundance of low kinetic energy product ions in the $m/e=22$ channel is consistent with formation of the secondary ion ND_4^+ by reaction of the charge transfer product ion ND_3^+ with ND_3, especially at higher ND_3 pressures. The velocity of many of the ND_3^+ charge transfer products is reduced in the lab frame relative to the reactant ion beam as illustrated by Figs. 3 and 4. Furthermore, those product ions with the lowest velocities have the highest collision cross sections giving rise to the broad,

poorly defined TOF spectra for secondary products.

The TOF profiles show sensitivity to both collision energy and vibrational excitation of the reactant ion. Definitive conclusions, however, cannot be made concerning their information content at this point. We defer a detailed discussion of the TOF profiles to future work and concentrate on the relative cross sections and product branching ratios that can be derived from these data.

3. Relative cross sections

We determine relative cross sections for the different product channels by taking the ratio of the integrated TOF product ion spectra, obtained by single ion counting, to the integrated parent ion signal, obtained by digitizing the analog wave form. The relative cross section measurements allow us to see directly which channels are becoming hindered or enhanced as a function of either collision energy or vibrational excitation. Our cross section determinations are limited to relative measurements for several reasons. With our collision gas inlet configuration, the cell path length is poorly defined, and it is difficult to measure the pressure accurately in the collision region. In addition, the parent ion signal is too large to use single ion counting, so we do not have a direct measure of the number of parent ions, which would be required for determining absolute cross sections. In future work we believe we can calibrate our system using a reaction with a known absolute cross section, such as $Ar^+ + H_2$ (Ref. 19) or $Ar^+ + N_2$ (Ref. 73).

Figure 5 shows the relative cross sections of each of the primary product channels as a function of umbrella mode excitation of NH_3^+ for three center-of-mass collision energies. Clearly, the effects of vibrational excitation are strongest at the lowest collision energy, 1.0 eV, and are attenuated at higher collision energies. At 1.0 eV deuterium abstraction [Fig. 5(a)] is enhanced by a factor of 3 in going from $\nu_2=0$ to $\nu_2=7$ in the umbrella mode. The charge transfer channel [Fig. 5(b)] increases by nearly a factor of 2, whereas proton transfer [Fig. 5(c)] is reduced by a factor of 2 as the excitation in ν_2 is increased from $\nu_2=0$ to $\nu_2=7$. At 5.0 and 10.0 eV collision energies both deuterium abstraction and charge transfer show a small increase with increasing vibrational excitation in the umbrella mode. The proton transfer channel decreases slightly with vibrational excitation at 5.0 eV and is constant at 10.0 eV.

Figure 6 displays the effect of center-of-mass collision energy on the relative reaction cross sections for the three product channels when NH_3^+ is prepared in $\nu_2=0$, 3, and 7. With only the zero-point vibrational energy in $NH_3^+(\nu_2=0)$, the relative cross sections for charge transfer yielding ND_3^+ and for deuterium abstraction yielding NH_3D^+ are almost unaffected by increasing the collision energy from 0.5 to 10.0 eV. In contrast, the proton transfer channel (ND_3H^+) decreases sharply by over a factor of 10 for the same collision energy range. As excitation of the umbrella mode in the reagent NH_3^+ ion is increased, charge transfer and deuterium abstraction show more dependence on collision energy; however, the proton transfer channel continues to show the strongest dependence.

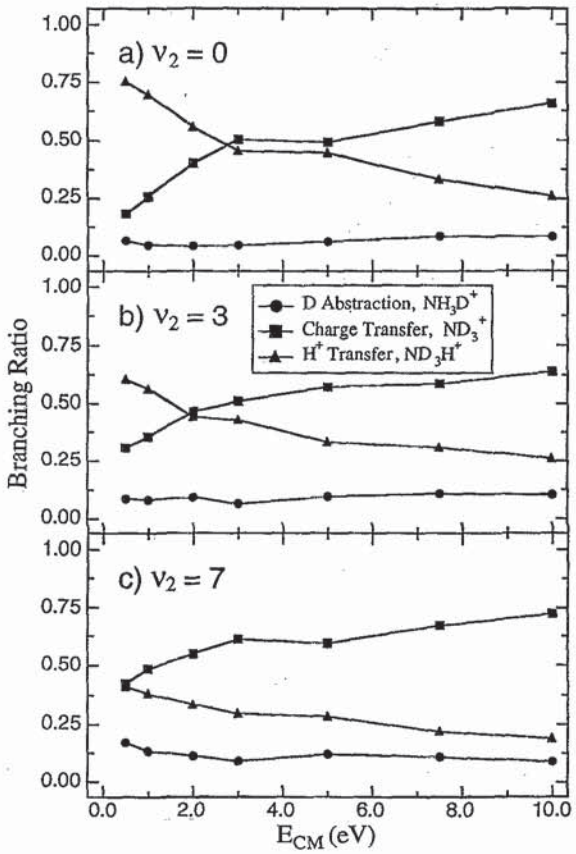

FIG. 8. Product branching ratios for the reaction $NH_3^+(\nu_2)+ND_3$ plotted as a function of the center-of-mass collision energy ($E_{c.m.}$) for three umbrella mode excitations, $\nu_2=0$, 3, and 7.

4. Product branching ratios

Product branching ratios are also determined from the integrated TOF profiles. Figure 7 shows product branching ratios at three collision energies plotted as a function of vibrational excitation in the umbrella mode of the reactant ion. These plots indicate a marked dependence on both vibrational excitation and collision energy. At the lowest collision energy of 1.0 eV [Fig. 7(a)], the sensitivity to vibrational excitation is greatest. At the highest collision energy [Fig. 7(c)] little or no effect is evident as excitation in the umbrella mode is increased. Evidently, the energy contributed to the reaction complex by translational energy overwhelms the initial vibrational excitation of the ion. At collision energies of 5 eV or less, deuterium abstraction and charge transfer are enhanced by excitation of the ν_2 mode in NH_3^+, whereas proton transfer is suppressed.

The product channel branching ratios are also sensitive to collision energy, as shown in Fig. 8. At the lowest collision energies, proton transfer is the strongest channel. As the collision energy is increased, charge transfer, which is negligible under thermal conditions ($k \lesssim 4\times10^{-11}$ cm^3 s^{-1}) relative to proton transfer and deuterium abstraction ($k=1.8\times10^{-9}$ cm^3 s^{-1}),[49] becomes the dominant channel. Interestingly, the collision energy at which the branching fractions for proton transfer and charge transfer are equal is

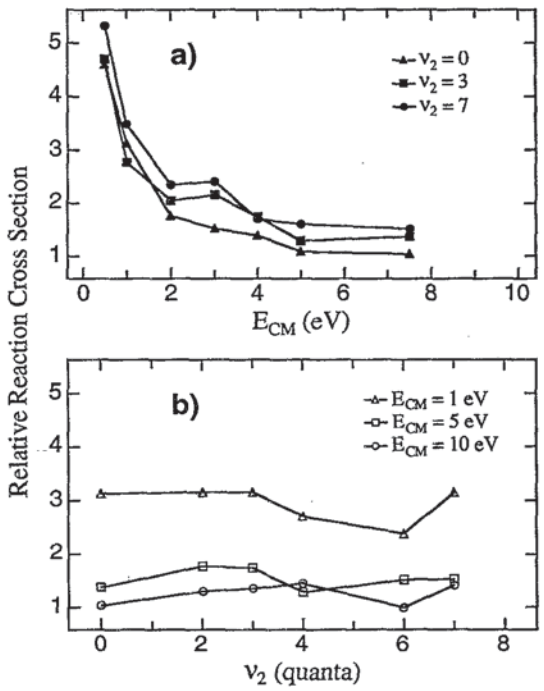

FIG. 9. Summed relative cross sections for the primary reaction channels, deuterium abstraction, charge transfer, and proton transfer, plotted as a function of (a) center-of-mass collision energy, $E_{c.m.}$ and (b) vibrational quanta in the umbrella mode (ν_2) of the NH_3^+ reagent.

lowered as the vibrational excitation of the reagent ion increases. At all collision energies deuterium abstraction is a relatively small channel accounting for less than 20% of the product ions. In addition, at high collision energies and high vibrational excitation the proton-transfer branching ratios approach the deuterium-abstraction branching ratios.

5. Relative cross section for all product channels

Figure 9 shows the relative reaction cross section summed over the three major product channels plotted as a function of both the center-of-mass collision energy and vibrational excitation. The total reaction cross section drops sharply as a function of collision energy [Fig. 9(a)]. At collision energies below 1 eV, this decrease is typical of Langevin behavior. Figure 9(b) displays the relative cross section for three different collision energies as a function of the number of quanta in the ν_2 umbrella mode. The total relative cross sections at a fixed collision energy are independent of vibrational excitation. Thus, the magnitude of the total cross section appears to be controlled by the collision energy rather than the degree of internal excitation of the reagent ion, consistent with the Langevin model for ion-molecule collisions that treats the ion as a point charge.[74] The reagent ion vibrational excitation does influence, however, the branching between product channels

IV. DISCUSSION

We have determined relative cross sections and product branching ratios for the reaction $NH_3^+(\nu_2=0-7)+ND_3$ at collision energies ranging from 0.5–10.0 eV c.m. Although the three major product channels for this reaction [Eq. (2)] reflect simple processes of electron or atom (H^+ or D) transfer, a complex interplay takes place between the reaction channels. Several significant trends are observed in these data. The relative cross sections for deuterium atom abstraction and charge transfer both increase with vibrational excitation of the ionic reagent, while proton transfer decreases (Fig. 5). The relative cross sections for the three major product channels decrease with increasing collision energy, just as the Langevin capture cross section behaves. Proton transfer exhibits a much more pronounced decrease with increasing collision energy than the other two channels (Fig. 6). From the product branching ratios we find that the branching fraction in the smallest channel, deuterium abstraction, increases slightly with vibrational excitation and that high collision energy and vibrational excitation favor charge transfer over proton transfer.

A. Comparison with previous work

One objective in this work was demonstration of the performance of our quadrupole-octopole-quadrupole mass spectrometer. The study that compares most directly with our work is that of Conaway *et al.*[44] Our experimental results show qualitative agreement with the trends observed for each reaction channel by Conaway *et al.* in their study of $NH_3^+(\nu_2)+ND_3$ using a tandem quadrupole mass spectrometer with a static collision cell. A notable difference between the two data sets is that we observe an enhancement of deuterium abstraction by a factor of ~3 in going from $\nu_2=0$ to $\nu_2=7$ at 1.0 eV, whereas Conaway *et al.* saw enhancement by as much as a factor of 4.5. In both experiments the enhancement of the deuterium abstraction channel diminishes with increasing collision energy. The inhibition of proton transfer in the two experiments was similar, roughly a factor of 2 in both cases. In the work of Conaway *et al.* the dependence of the relative cross section for proton transfer on vibrational excitation disappears within experimental error at collision energies above 8 eV; similar results were observed in our work [Fig. 5(c)]. Charge transfer increased by a factor of 1.5 in both experiments over the range of $\nu_2=0-7$ excitation. The enhancement of the charge transfer cross section was observed by Conaway *et al.* at all collision energies (2–12 eV). In our work the enhancement of charge transfer with vibrational excitation ($\nu_2=0-7$) is clearest at low collision energies [Fig. 5(b)]; some enhancement, although reduced, is present at higher collision energies.

Conaway *et al.*[44] observed that neutral atom abstraction was the dominant product channel, contrary to all previous work on this reaction system; they attributed this behavior to discrimination in product detection. Qualitative interpretation of our TOF profiles (Figs. 3 and 4) for the three major product channels provides insight into the results of Conaway *et al.* Our TOF distributions clearly show why NH_3D^+ was detected more efficiently than the other ionic products in these earlier experiments. The velocities of NH_3D^+ products in the lab frame are virtually unchanged from the velocity of the reagent ion beam. In contrast, the TOF profiles for the proton and charge transfer products have low kinetic energy

tails in the laboratory frame. The discrimination in product ion detection prevented direct comparison of the influence of vibrational excitation and collision energy on the branching between the three major product channels as well as the dependence of the relative cross section on collision energy. As a result, it is not possible to make further comparisons between our work and the work of Conaway *et al.*

Tomoda *et al.*[45(a)] report relative cross sections and product branching ratios for $NH_3^+(\nu_2)+ND_3$ and $ND_3^+(\nu_2)+NH_3$ obtained using the TESICO technique. Our product branching ratios show good agreement with their data at low collision energies ($\leqslant$3.1 eV) and significant deviations at higher collision energies. Anderson and co-workers[75] have seen similar discrepancies at high collision energies between cross sections and product branching ratios measurements made using guided ion beam techniques and the TESICO measurements of Honma *et al.*[76] for the system $C_2D_2^+(\nu_2)+H_2$ made using the same apparatus used by Tomoda *et al.*[45(a)] Anderson and co-workers carried out measurements for the $C_2H_2^+ + D_2$ reaction on two different guided ion beam instruments and found good agreement in both sets of experimental data. The most probable explanation for the disagreement at high collision energies is discrimination in product ion collection at higher energies in the TESICO apparatus.

Other studies have investigated the role of reagent excitation in the symmetric system: $NH_3^+(\nu_2)+NH_3$. Care must be taken in comparing results from the symmetric system with our data because hydrogen atom abstraction and proton transfer are indistinguishable and the symmetric system has the additional channel of *resonant* charge transfer. Chupka and Russell[37] observed that the cross section for NH_4^+ formation decreased at $\nu_2=9$ by a factor of 2 relative to $\nu_2=0$ at several collision energies. The decrease in the relative cross section for NH_4^+ production over the same internal energy range measured at thermal collision energies by van Pijkeren[43] was not as great (factor of 1.4). In our work the sum of the relative cross sections for deuterium abstraction and proton transfer at 1.0 and 5.0 eV decreases by factors of 1.4 and 1.2, respectively, from $\nu_2=0$ to $\nu_2=7$. In PIPECO experiments Baer and Murray[51] found that NH_4^+ formation was inhibited by umbrella mode excitation and that this effect increased with collision energy over the range 0.1–1.0 eV. At 1.0 eV a decrease in the relative cross section by a factor of 10 over the range $\nu_2=0$–9 was observed. In the same study charge transfer was enhanced by a factor of 2.4–2.6 at $\nu_2=9$ relative to $\nu_2=0$ at collision energies from 1.0–10.0 eV. In our work the enhancement of charge transfer with vibrational excitation is only a factor of 1.5. The differences between our data and that of Baer and Murray may reflect the influence of resonant charge transfer which is expected to play an important role in the symmetric system. Interestingly, in the work of Baer and Murray the effect of vibrational excitation is most pronounced at higher collision energies, in marked contrast with our observations that the influence of vibrational excitation appears to be "washed out" at higher collision energies. We have also noted that the branching between charge transfer and heavy particle (proton and atom) transfer is much more heavily weighted towards charge transfer in the work of Baer and Murray than in ours. We do not know the origin of this behavior.

Thus, our measurements seem to be in good overall agreement with those of other workers where direct comparisons can be made. We believe these comparisons give us confidence that our new quadrupole-octopole-quadrupole mass spectrometer can provide reliable data on state-selected ion-molecule reactions.

B. Nature of the collision complex

One of the major conclusions that can be drawn from our study of the influence of vibrational excitation and collision energy on the reaction of $NH_3^+(\nu_2)+ND_3$ is that this reaction does not proceed through a long-lived collision complex. Chesnavich and Bowers[48] were the first to predict a short-lived intermediate complex for this system when statistical phase space calculations showed poor agreement with the dependence of NH_4^+ formation on vibrational excitation observed by Chupka and Russell.[37] In attempting to model experimental data at thermal collision energies as a function of vibrational excitation, van Pijkeren *et al.*[43] concluded that a limited number of degrees of freedom participated in energy redistribution within the collision complex, consistent with a short lifetime. Our relative cross section and product branching ratio measurements as well as the raw time-of-flight data confirm this picture of a short-lived complex.

Collision energy and vibrational excitation play inequivalent roles in this reaction. Figure 9 clearly shows that collision energy controls the total cross section for the $NH_3^+(\nu_2)+ND_3$ reaction, whereas vibrational excitation apparently has no effect. The AADO theory,[74] which models NH_3^+ as a point charge, is able to predict the thermal rate constant within experimental error. If AADO theory also applies to this reaction at higher collision energies, then the total reaction rate constant would be expected to be independent of the internal energy of the ionic reagent. In addition to controlling the collision cross sections, translational energy contributes to the internal energy of the collision complex. From Figs. 7 and 8 it is apparent that an increase in the energy available to the collision complex either through vibrational excitation of the NH_3^+ reagent ion or from greater translational energy of the reagent ion enhances the charge transfer branching fraction and reduces the proton transfer branching fraction. The point at which the branching ratio for charge transfer crosses that for proton transfer in Figs. 7 and 8 provides some insight on the relative effectiveness of vibrational excitation and collision energy in supplying energy to the collision complex. Collision energy is roughly one-third as effective in energizing the collision complex as vibrational excitation. In a sufficiently long-lived complex both collision energy and reagent vibrational excitation are expected to be statistically redistributed within the collision complex, which implies that total energy rather than a specific type is important in determining the reaction outcome. This behavior is in contrast to our results.

In addition, if the reaction proceeds through a long-lived complex, an electron can be transferred many times between the nonbonding orbitals of the NH_3 and ND_3 moieties during the complex lifetime. Such rapid electron exchange removes

the distinction between the charged and neutral reagents. The resulting NH_3D^+ and ND_3H^+ branching ratios would be equal, each having contributions from neutral atom (H/D) abstraction and H^+/D^+ transfer. At the collision and internal energies investigated, branching fractions into the apparent proton transfer and deuterium abstraction channels, ND_3H^+ and NH_3D^+, are not equivalent. Only at high collision energies ($\geqslant$10 eV) do the branching fractions for the two heavy-particle transfer channels begin to approach each other. Other evidence expected for a long-lived complex is isotopic scrambling of the products, namely, the appearance of $NH_2D_2^+$, NH_2D^+, and ND_2H^+. Unfortunately these products cannot be distinguished by mass from the primary products.

The product TOF data (Figs. 3 and 4) provide additional support for the view that the reaction complex for this system is short lived. The TOF profile for the deuterium atom abstraction channel NH_3D^+ is sharply peaked and not significantly broader than the profile for the unreacted NH_3^+ beam, suggesting little perturbation of the NH_3^+ ion beam velocity in the process of picking up a deuterium atom from the thermal ND_3 collision gas. In contrast, the TOF profiles for charge transfer and proton transfer are much broader with low kinetic energy tails. Qualitatively, it appears that the majority of the product ions have slower velocities than the center of mass. One interpretation of this observation is that the product ion in charge transfer and proton transfer have motion characteristic of the thermal neutral reagent, that is, the collision complex does not live long enough for the full momentum of the ion beam to be transferred. To go beyond the current qualitative interpretation of the TOF data, further analysis must be carried out, namely, we must convert from TOF to kinetic energy in the c.m. frame.

It is not surprising that the reactive collision complex is short lived based on the energetics of the $NH_3^+ + ND_3$ system. At the lowest collision energy, 0.5 eV c.m., and no vibrational excitation of the reagents, the reagent energy is at least 1.29 eV above the entrance channel complex and 2.11 eV above the exit channel complex (Fig. 2). Without stabilizing collisions to remove some of the excess energy, the system cannot be trapped in either of these potential wells. Stabilization in the entrance channel would require a large barrier to product formation, which is ruled out because the reaction occurs on nearly every collision under thermal conditions. In addition, calculations by Radom and co-workers[65] predict that the barrier for formation of NH_4^+ is located 0.99 eV below the entrance channel. The absence of condensation products is consistent with a short-lived collision complex.

C. Models

1. Heavy-particle transfer

Several models have been proposed to rationalize the behavior of the $NH_3^+ + NH_3$ system and its isotopically labeled variants, particularly, the dependence of product formation on reagent ion vibrational excitation. The earliest work[37] on this ion-molecule reaction used unlabeled reagents and focused on the vibrational dependence of the NH_4^+ product channel. Formation of this product was attributed to proton transfer, which subsequent studies have verified to be the major heavy-particle transfer channel. In all the experimental work on this reaction, proton transfer was found to be inhibited by vibrational excitation in the umbrella mode (ν_2) of NH_3^+. The behavior of the proton transfer channel, Eq. (2c), has been explained by a direct model[44,45,48] in which a proton passes from the NH_3^+ ion to the central nitrogen atom in the neutral reagent [Fig. 10(b)]. Excitation of the umbrella mode results in motion orthogonal to the reaction coordinate for proton transfer. For a direct reaction, it might be expected that this process would be hindered by such motion resulting in a decrease in the relative cross sections as the umbrella mode excitation is increased. Our relative cross section results [Fig. 5(c)] are consistent with such a model, showing a factor of 2 decrease as excitation is increased from $\nu_2=0$ to $\nu_2=7$ at 1.0 eV.

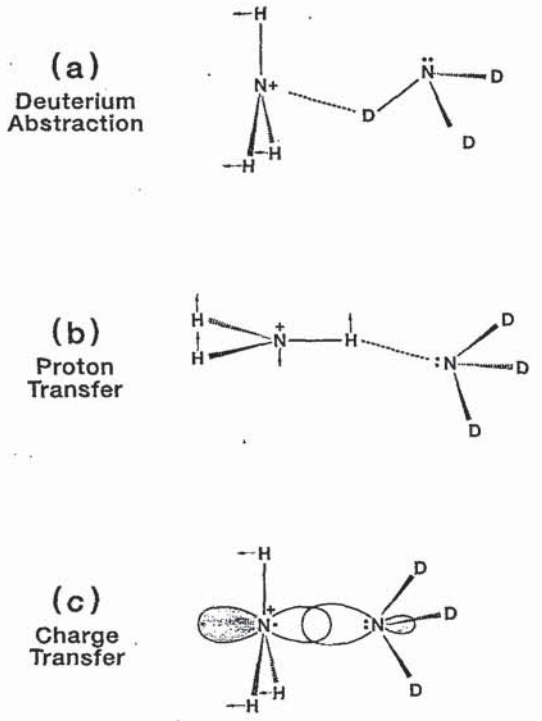

FIG. 10. Illustration of direct models for (a) deuterium abstraction, (b) proton transfer, and (c) charge transfer in the reaction $NH_3^+ + ND_3$.

Deuterium abstraction has been described alternately as either a one-step transfer of an atom or a two-step process consisting of electron transfer followed by proton transfer. The data do not allow us to distinguish between these two models. In the direct atom transfer model,[44,48] illustrated in Fig. 10(a), the umbrella bending motion is viewed as motion along the reaction coordinate. To bind a fourth H/D to the central nitrogen atom, the ion must bend from its planar equilibrium structure. In the reagent approach geometry shown for direct atom transfer [Fig. 10(a)], the orientation of the neutral dipole with respect to the ion is unfavorable; this provides a possible explanation for the small branching ratio ($\leqslant$20%) for this process. In contrast, the two-step model[45] attributes the enhancement in deuterium abstraction with increasing umbrella-mode excitation of NH_3^+ to promotion of

the initial charge transfer step by improved Franck–Condon overlap between the ion and neutral at higher values of ν_2. A possible argument against the two-step model is that if the electron can move between the two reagents on a time scale that is short compared to the collision complex lifetime, we would expect that proton transfer and deuterium abstraction would be equally probable. Only at high collision energies do the branching ratios for the two heavy-particle transfer channels begin to approach each other (Fig. 8). It is possible that electron exchange becomes important at higher collision energies. Whether deuterium abstraction proceeds by D transfer or by electron transfer followed by D^+ transfer, the vibrational excitation of the ν_2 umbrella mode of NH_3^+ seems to facilitate this channel by causing motion along the reaction coordinate. Perhaps studies of the reactivity and product branching ratios when NH_3^+ is prepared with excitation in different vibrational modes will allow a distinction to be made between these two models.

2. Charge transfer

Like deuterium abstraction, charge transfer is also enhanced by increasing the ν_2 vibrational excitation of the NH_3^+ ion. The branching ratio for this nearly thermoneutral reaction channel also increases sharply with collision energy. At thermal collision energies the rate constant for formation of the charge transfer product is 2 orders of magnitude smaller than the rate constant for heavy-particle transfer,[49] whereas at collision energies as low as 0.5 eV charge transfer accounts for over 15% of the reaction products. The symmetric charge transfer system, NH_3^+/NH_3, is doubly degenerate and, hence, the system will be split by the exchange interaction into a double-well potential energy surface for the ground electronic state, corresponding to charge localization on one of the ammonia moieties, and a single-well potential energy surface for the first excited state. At thermal collision energies the barrier between the two potential wells in the ground electronic state impedes transfer of the electron from the nonbonding orbital on the nitrogen atom of the neutral NH_3 to the half-filled nonbonding orbital on the nitrogen atom in NH_3^+. The nonsymmetric system also has a barrier to charge transfer; however, resonant charge transfer is not possible because of the vibrational frequency mismatch between NH_3/NH_3^+ and ND_3/ND_3^+. Both vibrational excitation and reagent translation can supply the energy to the system required to surmount this barrier.

Orbital overlap arguments suggest that an approach geometry in which the nonbonding orbital on the ion points toward the filled nonbonding orbital on the neutral would be most advantageous for electron transfer. This appears to be a favorable geometry for reagent approach because the dipole of the neutral is directed toward the charge. A number of investigators have suggested that the enhancement in charge transfer results from the increase in Franck–Condon overlap between the ion and neutral with increasing excitation in the umbrella mode;[45,51,77] however, the enhancement is smaller than expected if Franck–Condon overlap was the sole governing factor. The Franck–Condon factors increase 30 times in size in going from $\nu_2=0$ to $\nu_2=5$ in the umbrella mode. The enhancement of the charge transfer channel with increasing internal excitation of the ionic reagent and collision energy may simply reflect a shorter interaction time between the reagents; any reactive complex can fall apart after the electron jumps but before a heavier particle is transferred.

V. CONCLUDING REMARKS

The quadrupole-octopole-quadrupole mass spectrometer in combination with REMPI is a versatile tool for studying a variety of ion-molecule reaction systems. Our results on the $NH_3^+(\nu_2)+ND_3$ reaction demonstrate the performance of this instrument. The reaction of $NH_3^+(\nu_2)$ with ND_3 is characterized by three competing channels whose dynamics depend on vibrational excitation and translational energy of the reagent. Vibrational excitation and collision energy show differing efficiencies in delivering energy to the reaction. For this system simple ideas concerning motion along the reaction coordinate or orthogonal to it, taken from neutral reaction dynamics, offer a qualitative picture consistent with observations.

ACKNOWLEDGMENTS

This work was supported by the Air Force Office of Scientific Research under Grant No. AFOSR-89-0264. L.A.P. was supported by a National Science Foundation Postdoctoral Research Fellowship in Chemistry (CHE-8907493).

[1] S. L. Anderson, in *State-Selected and State-to-State Ion-Molecule Reaction Dynamics, Part I: Experiment*, edited by C.-Y. Ng and M. Baer (Wiley, New York, 1992), p. 177.
[2] T. Baer, in *Gas Phase Ion Chemistry*, edited by M. T. Bowers (Academic, New York, 1979), p. 153.
[3] C.-Y. Ng, in *Techniques for the Study of Ion-Molecule Reactions*, edited by J. M. Farrar and W. H. Saunders, Jr. (Wiley, New York, 1988), p. 417.
[4] S. T. Pratt, P. M. Dehmer, and J. L. Dehmer, J. Chem. Phys. **80**, 1706 (1984).
[5] W. E. Conaway, R. J. S. Morrison, and R. N. Zare, Chem. Phys. Lett. **113**, 429 (1985).
[6] T. Ebata and R. N. Zare, Chem. Phys. Lett. **130**, 467 (1986).
[7] T. M. Orlando, S. L. Anderson, J. R. Appling, and M. G. White, J. Chem. Phys. **87**, 852 (1987).
[8] M. N. R. Ashfold, B. Tutcher, B. Yang, Z. K. Jin, and S. L. Anderson, J. Chem. Phys. **87**, 5105 (1987).
[9] H. Park, P. J. Miller, W. A. Chupka, and S. D. Colson, J. Chem. Phys. **89**, 3919 (1988).
[10] B. Yang, M. H. Eslami, and S. L. Anderson, J. Chem. Phys. **89**, 5527 (1988).
[11] H. Park, P. J. Miller, W. A. Chupka, and S. D. Colson, J. Chem. Phys. **89**, 6676 (1988).
[12] J. Xie and R. N. Zare, Chem. Phys. Lett, **159**, 399 (1989).
[13] A. Fujii, T. Ebata, and M. Ito, Chem. Phys. Lett. **161**, 93 (1989).
[14] C.-L. Liao, J.-D. Shao, R. Xu, G. D. Flesch, Y.-G. Li, and C.-Y. Ng, J. Chem. Phys. **85**, 3874 (1986).
[15] J.-D. Shao, Y.-G. Li, G. D. Flesch, and C.-Y. Ng, J. Chem. Phys. **86**, 170 (1987).
[16] G. D. Flesch, S. Nourbakhsh, and C.-Y. Ng, J. Chem. Phys. **92**, 3590 (1990).
[17] J. Xie and R. N. Zare, J. Chem. Phys. **96**, 4293 (1992).
[18] S. L. Anderson, F. A. Houle, D. Gerlich, and Y. T. Lee, J. Chem. Phys. **75**, 2153 (1981).
[19] K. M. Ervin and P. B. Armentrout, J. Chem. Phys. **83**, 166 (1985).
[20] J.-D. Shao and C.-Y. Ng, Chem. Phys. Lett. **118**, 481 (1985).
[21] D. Gerlich, in *Electronic and Atomic Collisions*, edited by D. C. Lorents, W. E. Meyerhof, and J. R. Peterson (Elsevier, Amsterdam, 1986), p. 541.
[22] D. Gerlich, R. Disch, and S. Scherbarth, J. Chem. Phys. **87**, 350 (1987).
[23] D. Gerlich, in *State-Selected and State-to-State Ion-Molecule Reaction Dynamics, Part I: Experiment*, Ref. 1, p. 1.

[24] E. Teloy and D. Gerlich, Chem. Phys. **4**, 417 (1974).
[25] J.-D. Shao and C.-Y. Ng, J. Chem. Phys. **84**, 4317 (1986).
[26] S. Scherbarth and D. Gerlich, J. Chem. Phys. **90**, 1610 (1989).
[27] T. M. Orlando, B. Yang, and S. L. Anderson, J. Chem. Phys. **90**, 1577 (1989).
[28] T. M. Orlando, B. Yang, Y. Chiu, and S. L. Anderson, J. Chem. Phys. **92**, 7356 (1990).
[29] B. Yang, Y. Chiu, and S. L. Anderson, J. Chem. Phys. **94**, 6459 (1991).
[30] L. Hanley, S. A. Ruatta, and S. L. Anderson, J. Chem. Phys. **87**, 260 (1987).
[31] S. K. Loh, D. A. Hales, L. Lian, and P. B. Armentrout, J. Chem. Phys. **90**, 5466 (1989).
[32] S. A. Ruatta and S. L. Anderson, J. Chem. Phys. **89**, 273 (1988).
[33] S. K. Loh, L. Lian, and P. B. Armentrout, J. Chem. Phys. **91**, 6148 (1989).
[34] P. A. Hintz, S. A. Ruatta, and S. L. Anderson, J. Chem. Phys. **92**, 292 (1990).
[35] K. Kimura, S. Katsumata, Y. Achiba, T. Yamazaki, and S. Iwata, *Handbook of He I Photoelectron Spectra of Fundamental Organic Molecules* (Japan Scientific Societies Press, Tokyo, 1981), p. 42.
[36] P. Botschwina, J. Chem. Soc., Faraday Trans. 2 **84**, 1263 (1988).
[37] W. A. Chupka and M. E. Russell, J. Chem. Phys. **48**, 1527 (1968).
[38] J. L. Franklin and M. A. Haney, J. Phys. Chem. **73**, 2857 (1969).
[39] W. T. Huntress, Jr. and R. F. Pinizzotto, Jr., J. Chem. Phys. **59**, 4742 (1973).
[40] R. S. Hemsworth, J. D. Payzant, H. I. Schiff, and D. K. Bohme, Chem. Phys. Lett. **26**, 417 (1974).
[41] W. Lindinger, D. L. Albritton, F. C. Fehsenfeld, A. L. Schmeltekopf, and E. E. Ferguson, J. Chem. Phys. **62**, 3549 (1975).
[42] S. T. Ceyer, P. W. Tiedemann, B. H. Mahan, and Y. T. Lee, J. Chem. Phys. **70**, 14 (1979).
[43] D. v. Pijkeren, J. v. Eck, and A. Niehaus, Chem. Phys. **95**, 449 (1985).
[44] W. E. Conaway, T. Ebata, and R. N. Zare, J. Chem. Phys. **87**, 3453 (1987).
[45] S. Tomoda, S. Suzuki, and I. Koyano, J. Chem. Phys. **89**, 7268 (1988); (b) H. Tachikawa and S. Tomoda, Chem. Phys. **182**, 185 (1994).
[46] T. Su, E. C. F. Su, and M. T. Bowers, J. Chem. Phys. **69**, 2243 (1978).
[47] N. G. Adams, D. Smith, and J. F. Paulson, J. Chem. Phys. **72**, 288 (1980).
[48] W. J. Chesnavich and M. T. Bowers, Chem. Phys. Lett. **52**, 179 (1977).
[49] W. T. Huntress, Jr., M. M. Mosesman, and D. D. Elleman, J. Chem. Phys. **54**, 843 (1971).
[50] L. W. Sieck, L. Hellner, and R. Gorden, Jr., Chem. Phys. Lett. **10**, 502 (1971).
[51] T. Baer and P. T. Murray, J. Chem. Phys. **75**, 4477 (1981).
[52] R. D. Guettler, G. C. Jones, Jr., L. A. Posey, N. J. Kirchner, B. A. Keller, and R. N. Zare, J. Chem. Phys. **101**, 3763 (1994), preceding paper.
[53] J. W. Farley, Rev. Sci. Instrum. **56**, 1834 (1985).
[54] B. A. Huber, T. M. Miller, P. C. Cosby, H. D. Zeman, R. L. Leon, J. T. Moseley, and J. R. Peterson, Rev. Sci. Instrum. **48**, 1306 (1977).
[55] H. D. Zeman, Rev. Sci. Instrum. **48**, 1079 (1977).
[56] G. Mauclaire, M. Heninger, S. Fenistein, J. Wronka, and R. Marx, Int. J. Mass. Spectrom. Ion Proc. **80**, 99 (1987).
[57] R. J. S. Morrison, W. E. Conaway, and R. N. Zare, Chem. Phys. Lett. **113**, 435 (1985).
[58] R. J. S. Morrison, W. E. Conaway, T. Ebata, and R. N. Zare, J. Chem. Phys. **84**, 5527 (1986).
[59] W. E. Conaway, T. Ebata, and R. N. Zare, J. Chem. Phys. **87**, 3447 (1987).
[60] P. J. Chantry, J. Chem. Phys. **55**, 2746 (1971).
[61] R. H. Neynaber, J. A. Rutherford, and D. A. Vroom, Gulf Radiation Technology Report No. Gulf-RT-A12209 (DNA 2944F), July 1972.
[62] W. Kamke, R. Herrmann, Z. Wang, and I. V. Hertel, Z. Phys. D **10**, 491 (1988).
[63] J. C. Greer, R. Ahlrichs, and I. V. Hertel, Z. Phys. D **18**, 413 (1991).
[64] W. J. Bouma and L. Radom, J. Am. Chem. Soc. **107**, 345 (1985).
[65] P. M. W. Gill and L. Radom, J. Am. Chem. Soc. **110**, 4931 (1988).
[66] N. Ganghi, J. L. Wyatt, and M. C. R. Symons, J. Chem. Soc., Chem. Commun. **1986**, 1424 (1986).
[67] S. Tomoda, Chem. Phys. **110**, 431 (1986).
[68] S. Tomoda, Faraday Discuss. Chem. Soc. **85**, 53 (1988).
[69] S. Tomoda and K. Kimura, in *Vacuum Ultraviolet Photoionization and Photodissociation of Molecules and Clusters*, edited by C.-Y. Ng (World Scientific, Singapore, 1991), p. 101.
[70] G. A. W. Derwish, A. Galli, A. Giardini-Guidoni, and G. G. Volpi, J. Chem. Phys. **39**, 1599 (1963).
[71] C. E. Melton, J. Chem. Phys. **45**, 4414 (1966).
[72] R. A. Dressler, J. A. Gardner, R. H. Salter, F. J. Wodarczyk, and E. Murad, J. Chem. Phys. **92**, 1117 (1990).
[73] R. I. Martinez and S. Dheandhanoo, Int. J. Mass Spectrom. Ion Proc. **84**, 1 (1988).
[74] T. Su and M. T. Bowers, in *Gas Phase Ion Chemistry*, edited by M. T. Bowers (Academic, New York, 1979), p. 83.
[75] S. L. Anderson (private communication).
[76] K. Honma, K. Tanaka, and I. Koyano, J. Chem. Phys. **86**, 688 (1987).
[77] T. Ebata, W. E. Conaway, and R. N. Zare, Int. J. Mass Spectrom. Ion Proc. **80**, 51 (1987).